Hippocampal Based Model Reveals the Distinct Roles of Dentate Gyrus and CA3 during Robotic Spatial Navigation

Diogo Santos Pata[1], Alex Escuredo[1],
Stéphane Lallée[1], and Paul F.M.J. Verschure[1,2]

[1] Universitat Pompeu Fabra (UPF), Synthetic, Perceptive, Emotive and Cognitive Systems group (SPECS)
Roc Boronat 138, 08018 Barcelona, Spain
http://specs.upf.edu
[2] Institució Catalana de Recerca i Estudis Avançats (ICREA)
Passeig Llus Companys 23, 08010 Barcelona, Spain
{diogo.pata,alex.escuredo,stephane.lallee,paul.verschure}@upf.edu
http://www.icrea.cat

Abstract. Animals are exemplary explorers and achieve great navigational performances in dynamic environments. Their robotic counterparts still have difficulties in self-localization and environment mapping tasks. Place cells, a type of cell firing at specific positions in the environment, are found in multiple areas of the hippocampal formation. Although, the functional role of these areas with a similar type of cell behavior is still not clearly distinguished. Biomimetic models of navigation have been tested in the context of computer simulations or small and controlled arenas. In this paper, we present a computational model of the hippocampal formation for robotic spatial representation within large environments. Necessary components for the formation of a cognitive map [1], such as grid and place cells, were obtained through attractor dynamics. Prediction of future hippocampal inputs was performed through self-organization. Obtained data suggests that the integration of the described components is sufficient for robotic space representation. In addition, our results suggest that dentate gyrus (DG), the hippocampal input area, integrates signals from different dorsal-ventral scales of grid cells and that spatial and sensory input are not necessarily associated in this region. Moreover, we present a mechanism for prediction of future hippocampal events based on associative learning.

Keywords: spatial navigation, cognitive map, hippocampus, place cells, CA3, dentate gyrus, robotics.

1 Introduction

Animals have the talent to alter their navigational method and plan optimized novel trajectories after environmental changes. It has been argued that animals form an internal cognitive map [1], which may potentiate rapid adaptation to

A. Duff et al. (eds.): Living Machines 2014, LNAI 8608, pp. 273–283, 2014.

their surroundings. The hippocampal formation in the medial temporal lobe of the mammalian brain has been associated with learning, memory and spatial navigation. Since the discovery of place cells [2], a type of cell showing firing activity at unique positions (place fields) of the explored environment, these type of cell have been considered to be the building blocks of the animals cognitive map. Place cells are found in the dentate gyrus (DG), CA3 and CA1 regions of the hippocampus. The formation of place cells is thought to be the result of summation and association of earlier inputs. Medial (MEC) and lateral (LEC) entorhinal cortex (EC) areas, one synapse upstream from hippocampus, feed the hippocampal formation with spatial (motion) and processed sensory information, respectively. Grid cells, a type of cell found in MEC layer II and III, spike at multiple positions of the explored environment and present a specific triangular tessellation pattern when plotted over space. Grid cells are considered the metric system needed for building a spatial representation of space. As described in [3], grid cells scale up progressively from the dorsal to ventral part of MEC. That is, the spacing between cells firing fields increase along the dorsal-ventral axis. In combination, MEC and LEC cells provide the hippocampus with specific information about the animal position. The DG is the input region of the hippocampus, receiving excitatory signals from EC layer II through the so-called perforant pathway. This pathway is divided into medial and lateral paths, each of them carrying signals from MEC and LEC respectively. The medial perforant path projects onto the middle one-third of the DG molecular layer, while the lateral perforant path terminates in the outer one-third of the DG molecular layer [4]. Consequently, the DG projects signals to the CA3 area. The CA3 region receives input from granule cells in the DG and from EC layer II cells. The extensive collateral ramification of CA3 pyramidal cells [5], make it a suitable network for associative memory and learning processes. It has been shown that both DG and CA3 areas contain cells which sensitivity is specific to unique positions of the environment. However, the roles for DG and CA3 areas in spatial navigation are still poorly distinguished. In this paper, we hypothesize two different roles for DG and CA3 during navigational tasks. On one hand, DG integrates multiple information arriving from different levels of the dorsal-ventral axis of MEC, but does not necessarily mix outer and middle one-third layer signals. However, DG is still capable of presenting position specific activity. On the other hand, CA3 region acts as an associative network, integrating motion and sensory signals, and is capable of performing spatial and sensory predictions. With that in mind, we have developed a computational model of the EC-DG and EC-CA3 connections and tested it on a mobile robot.

2 Methods

We construct a set of neural populations resembling the activity of each of the components of our system, namely: MEC, DG and CA3. Grid cells (MEC) were built through attractor mechanisms on a toroidal network as described in [6]. Specific evidence of continuous attractor dynamics in grid cells has been shown

physiologically [7] which make attractor models a plausible mechanism for generating the behavior of such cell. Four sub-populations of grid cells with different gains (0.09; 0.07; 0.05 and 0.03), thus progressively bigger grid scales, were categorized as: Dorsal, Medial-1, Medial-2 and Ventral, respectively (see figure 2 and 4). As in [6], synaptic weights were updated accordingly with the robot movement, bumping the activity in a direction based on the robot's movement direction DG population was defined as a matrix of N neurons with equal size as MEC networks. The neurons of the network are initialized by

$$A_j = \frac{\sum_{c=1}^{M} A_c}{M} \tag{1}$$

where the activity of each neuron j is determined by the average sum of activity in the correspondent network position for every grid cell network, being M the amount of grid cell networks projecting to DG (see figure 1). A low-dimensional continuous attractor mechanism was implemented in the DG network, and it is initialized after MEC signals arrive to DG (figure 1). Given that DG network has an all-to-all type of connectivity, the activity of each cell at time t + 1, i.e. *A_i(t+1)*, in between MEC arrivals, is defined by

$$A_i(t=1) = \sum_{i=1}^{N} A_j(t) w_{ij} \tag{2}$$

where N is the number of neurons in the network and w_{ij} is the synaptic weight connecting cell j to cell i, with i, $j \in \{ 1, 2, ..., N\}$.The synaptic strength is defined by the Gaussian weight function

$$W_{ij} = I_{exp}\left(\frac{||c_i - c_j||^2}{\sigma^2}\right) - T \tag{3}$$

where $c_i = (c_{i_x}, c_{i_y})$ is the Cartesian position of the cell i in the network (with $i_x \in \{ 1, 2, ..., N_x \}$ and $i_y \in \{ 1, 2, ..., N_y\}$), and where N_x and N_y are the number of columns and rows in the network. As in [6], the strength of the synapses is defined by the parameter I, whereas σ is the size of the Gaussian and T is the shift parameter defining excitatory and inhibitory zones. Contrary to [6], the norm $\|.\|^2$ is the Euclidean distance between cell i and cell j in non-periodic boundary conditions (see table 1).

Because MEC and DG show theta- and gamma-frequencies [8] [9], we scaled the update time for each population accordingly with their oscillatory frequency, 4-12Hz and 30-90Hz, respectively (see figure 1 bottom-right). That is, the DG attractor cycle was set to update fourteen times faster than MEC signal arrivals. This time delay is sufficient for the activity in DG to be attracted towards a stable point. Every time MEC networks project onto DG, the later is reset and updated conformably equation 1. Attractor models have been used to model place cells in the DG (see [10], for example). Their type of attraction is based on the animal movement, such as the previously described mechanism of attraction

Table 1. Values of the parameters used in DG model

Parameter	Value	Unit
N	100	[cell]
N_x	10	[cell]
N_y	10	[cell]
I	0.3	[no unit]
σ	0.36	[meter]
T	0.05	[no unit]

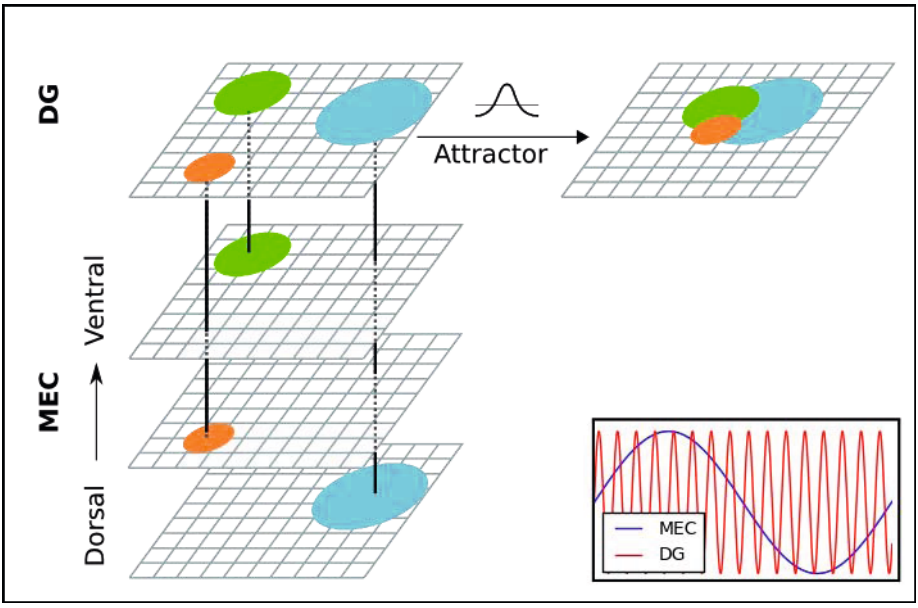

Fig. 1. Place cells attractor mechanism. The DG integrates input from multiple MEC grid cell networks at different scales of the dorsal-ventral axis. The attractor bumps network activity to a single point. Bottom-right: Every time the oscillation reaches its maximum a time step is performed in its network. The higher frequency in the DG relative to MEC ensures that the DG attractor updates in between MEC arrivals.

for grid cell generation in MEC layer II (see [6]). However, attractor models do not describe the characteristics of DG cells. Contrary to those models, place cells do not present a topographical organization. Also, such models do not take into account MEC inputs. Instead, they reproduce a grid cell activity with a grid scale sufficiently large to fire at a single position of the environment. Thus, the gain factor, a parameter modulating the spacing between firing fields, needs to be defined in accordance with the size of the arena. To validate the hypothesis that CA3 accounts for a hippocampal input prediction mechanism, we used the Convergence Divergence Zone Framework as described in [11] to learn

associations of the input space. This framework, based on the self-organizing map algorithm, is trained through unsupervised learning, generating low-dimensional representations of multiple inputs. Since CA3 region receives input from both lateral and medial areas of the entorhinal cortex, and is thought to be a highly associative type of network, we projected grid cell network and visual (sensory) signals onto our CA3 network. Thus, error prediction can be quantified by the difference between expected and real inputs.

In order to validate the hypothesis that place cells in the DG emerge through the integration of multiple MEC inputs, and that associative networks in the CA3 area account for hippocampal input prediction, we implemented the described system on a mobile robot setup (Figure 2) and tested it in a 3x4 meters open arena, during 45 minutes. The robot was programmed to randomly explore the environment, using its proximity sensors to avoid collision with walls. Visual input was obtained through a fixed wireless camera placed in the front of the robot. Given that sensory information is highly processed when it arrives to LEC areas, we simulated such processing by applying an edge-detection algorithm to the visual input before it is projected to CA3. LEC network activity was simulated from a one-to-one mapping of the pixel activity in the filtered visual input matrix in normalized gray-scale with dimensions of 100x100 pixels. The AnTs video tracking system [12] tracked the robots position during the whole session. The robots orientation was obtained from the tracking system and used to feed grid cell networks. Two 32bits computers (Linux Ubuntu 13.10 and Windows XP) were connected to the system network and used to run the system components. The system was developed using C++ and Python programming languages, and system connections were established through the YARP middleware [13]. During robot spatial exploration, grid cell networks (MEC) projected their activity to both DG and CA3 populations, while filtered visual inputs only projected to CA3.

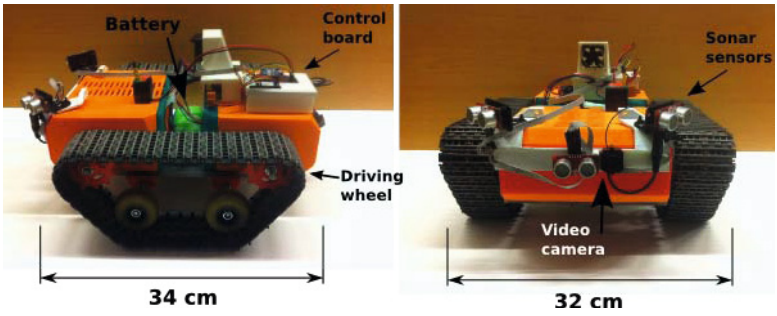

Fig. 2. Robotic platform. Left: side view; right: front view. Two bidirectional continuous track wheels sustain the platform. Three sonar sensors placed in the front of the robot allow it to perform collision-avoidance. A wireless video camera records the robot visual field. A control board orchestrates sensory and motor signals.

3 Results

Grid cell activity from the multiple dorsal-ventral networks reveal the triangular tessellation pattern of their firing fields when plotted over the explored environment (figure 3 and 4). Grid scale and firing field size was in accordance with electrophysiological studies [3]. Grid cells belonging to different dorsal-ventral MEC axis presented a progressive increase in both grid scale and firing fields size (figure 4). These results show that the mechanism of grid cell generation based on attractor dynamics is sufficiently robust to generate the triangular tessellation pattern within large-scale environments.

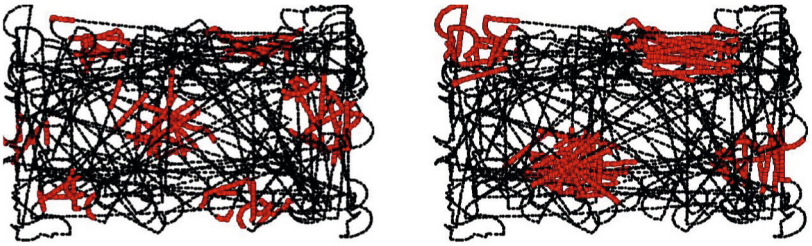

Fig. 3. Triangular tessellation pattern of two grid cells. Black dots represent the robots trajectory. Red dots represent positions where the cell activity was higher than 75 percent of its maximum activity. Left: Medial-1 grid cell. Right: Medial-2 grid cell.

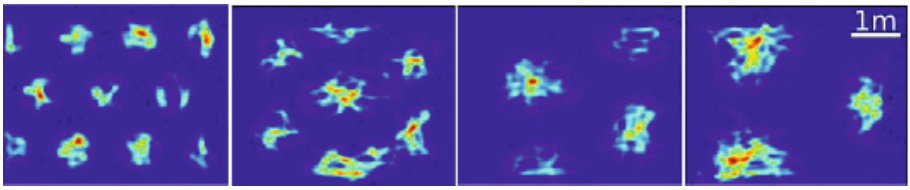

Fig. 4. Autocorrelogram of four grid cells from each dorsal-ventral level. From left to right: Dorsal, Medial-1, Medial-2, Ventral.

After validation of the grid cell networks behavior, we questioned whether the proposed model of DG based on integration and attraction mechanisms would account for place cell generation. Indeed, when plotted over space, the activity of DG network cells reveal sensitivity to specific positions of the environment (figure 5). Contrary to grid cells, no scale or firing field size pattern was observed. We must notice that no homogeneous shape of the firing field was observed. Indeed, different cells can have completely different firing field characteristics. For instance, cell 87 in figure 5 has a much broader place field when compared with cell 15 of the same figure. Another interesting feature of our models DG

place cells is that despite being sensitive to certain positions of the explored environment, the number of positions to which they are sensitive to, vary from cell to cell. In order to quantify the amount of place fields to which each cell reacts, an iterative hierarchical clustering algorithm analyzed all data points, in x-y coordinates, that presented activity superior to 75 percent of the cells higher activity. The clustering threshold rule was determined to the maximum of 30 percent (150cm) of the environment maximum length (500cm). Clustering results (figure 7) indicate that 52 percent of the cells in this network are sensitive to one single position of the environment, while 28 percent encode sensitivity in two regions of the environment. Silent cells, a type of cell that do not spike significantly at any position of the environment, constitute 12 percent of the neural population. A few amount of cells, 8 percent, present sensitivity at 3 or 4 different regions.

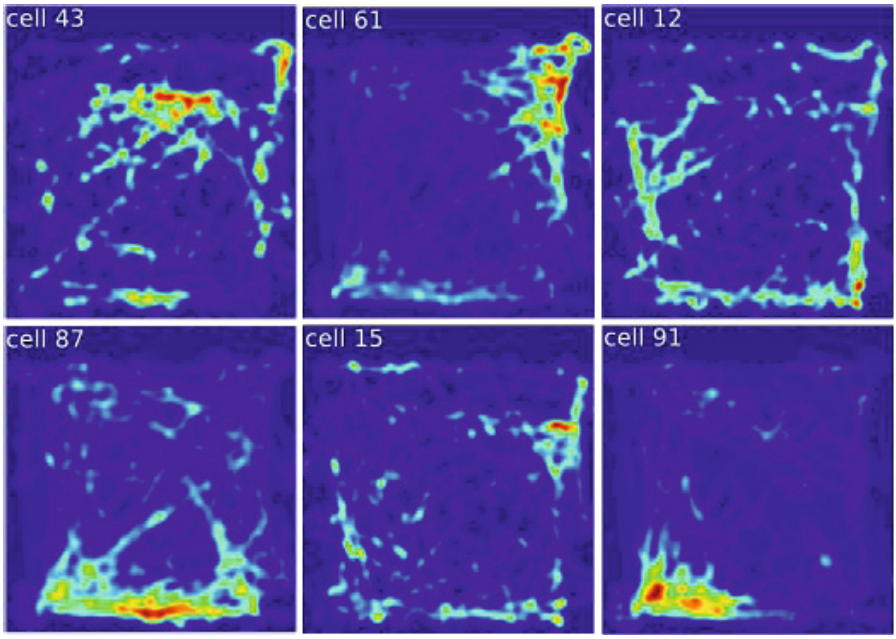

Fig. 5. Dentate gyrus place cells activity autocorrelogram.Place fields of six cells.

To further validate the role of CA3 during navigational tasks, we tested whether our CA3 model accounts for spatial encoding as it happens in the same region of the mammalian brain. As for DG, CA3 cells are also revealed to be spatially sensitive. Cells become active accordingly to the robots position (figure 6). Indeed, when comparing with the distribution of DG cells per amount of place fields, CA3 cells shown to have more confined place fields. Results from the hierarchical clustering analysis shows that 71 percent of the cells are active

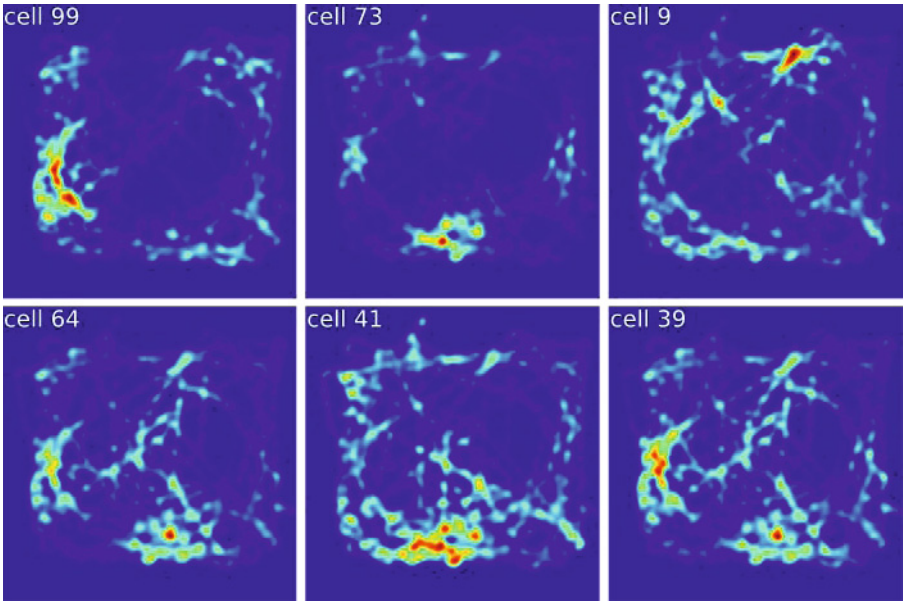

Fig. 6. CA3 place cells activity autocorrelogram. Place fields of six cells.

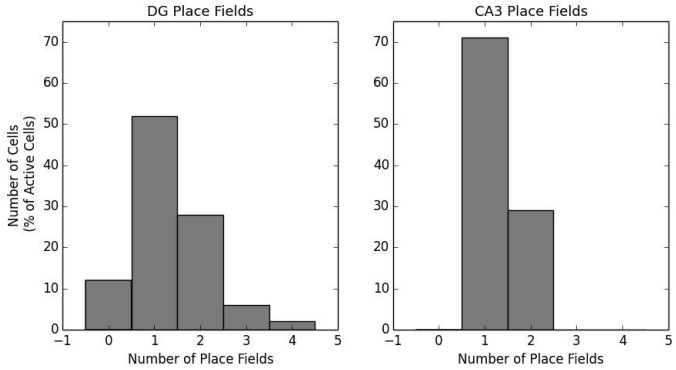

Fig. 7. Place fields distribution for both DG (left) and CA3 (right) networks. Results from hierarchical clustering.

at unique positions of the environment, while 29 percent are sensitive to two different positions (e.g. cell 39 in figure 6). Such results suggest that learned associations between MEC and LEC inputs are sufficient and accurate enough for place sensitivity.

Despite its role in place sensitivity and memory formation, we hypothesized that CA3 would account as a mechanism for hippocampal input prediction. To test this hypothesis, we projected MEC and LEC signals to the CA3 region

during robot exploration, aiming that the Convergence Divergence Zone Framework would learn associations from the input state and predict future inputs. As suggested by [14] for the DG, we used a substantially larger amount of MEC inputs into the CA3 than those of LEC. Specifically, 70 percent of signals associated in CA3 were provided by grid cell networks, while only 30 percent were projected from LEC. Quantification of the prediction error was performed by the difference, in percentage, between the real and the expected input for each modality (figure 7). Naturally, the error tends to decrease for every modality as the robot explores the arena. As we would expect, prediction error progressively decreases from dorsal to ventral grid cells input. The reason might be that more dorsal networks bump the activity around the cyclic network faster when compared with more ventral networks. With slower bumping movements of the activity, ventral networks tend to be more stable. Interestingly, the prediction error for the visual input stabilized faster than any other modality, but never reached the minimum of Medial-2 or Ventral errors. The fact the visual inputs are relatively stable and easily predicted when the robot moves straight but not when it turns, might explain why it stabilizes faster but does not improve after stabilization.

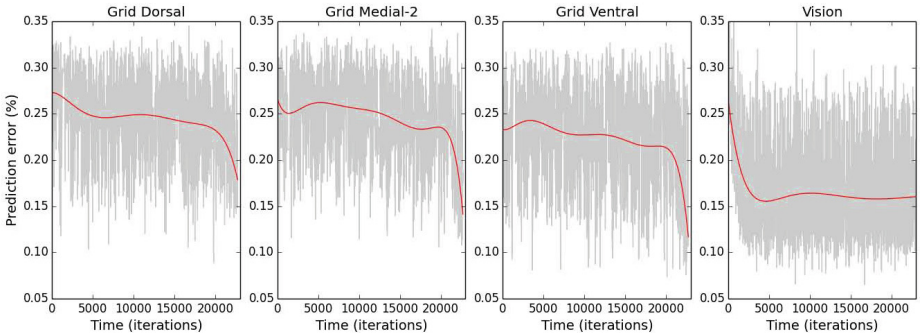

Fig. 8. Prediction error for each modality

4 Discussion

In this article, we have presented an integrated hippocampal model that accounts for spatial representation and input prediction, embedded on a real mobile agent. We have shown that a previously described model of grid cells based on attractor dynamics is sufficiently robust for generating the same cell behavior in a living machine navigating in a large environment. As previously shown in rats, the grid scale increased progressively from the dorsal to ventral areas of the MEC. We have tested the hypothesis that place cells in the DG are a result from the integration of multiple grid cell networks with different scales. To do that, we have presented a model of the DG place cells based on both integration of earlier projections and attractor mechanisms, in which the gating of inputs and network

dynamics work at different frequencies. A network of non-periodic boundaries conditions is reset with sparse activity every time that MEC networks project their inputs. Because the DG recurrently processes internal signals at a higher frequency than the frequency at which external signals arrive, the mechanisms of attraction are fast enough to stabilize activity at any given point in the network. We have shown that this model is capable of tuning the receptive field of each cell to specific positions of the environment. Specifically, 52 out of 100 cells were shown to be active at unique positions of the environment, while 28 were sensitive for two firing fields, and only 12 were considered to be silent cells. We have also hypothesized that even though both DG and CA3 hippocampal areas contain apparently similar types of cells (place cells), the role of CA3 during navigational tasks would not only be relevant for associative learning, but may also be crucial for prediction of future inputs. With that in mind, we tested a previously described associative learning framework within the context of CA3 input associations. The same grid cell networks used for the DG model were used in combination with processed visual input to feed the CA3 network. Results suggest that input error prediction tends to be smaller for grid cell inputs at the ventral areas when compared with dorsal areas. The fact that activity movements within the network are faster for dorsal than for ventral areas could explain why inputs are easier predicted for the later. Also, it is interesting that prediction error of visual input tends to stabilize significantly faster than those predictions of MEC inputs. However, stabilization is at a higher error value than posterior predictions of MEC. Despite the fact that visual input changes smoothly when the robot moves straight, which make it easier to predict, we should not discard the hypothesis that speed vector encoded by grid cells could be of great help for the visual prediction, but that visual information is poorer as a hint of grid cells space state. In conclusion, we have addressed the question whether roles of DG and CA3 during spatial navigation could be distinguished even though they show similar type of cells. To test whether DG place cells are part of an integration mechanism or not, we have built a new model of DG based on the attraction of signals arriving from MEC. Also, to verify that MEC and LEC associations not only show place sensitivity, but could also account for a prediction mechanism, we have used a previously described model of associative learning using inputs resembling those of hippocampal formation. Both models were tested on a mobile robot freely navigating in an open arena. Results suggest that integration of MEC signals in the DG are sufficient to generate place cells like type of activity but with lower precision than CA3 place cells. Also, when fed with hippocampal type inputs a map of self-organization was able to predict future states. To our knowledge, this was the first time that the question of role distinction in hippocampal areas with similar cell behavior has been addressed and explained with concrete neural mechanisms. Also, a novel attractor model for place cells in the DG built through MEC inputs and non-predefined gain values was presented. In future work, we plan to combine both DG and CA3 models as a mechanism for path integration correction. Closing the

entorhinal-hippocampal loop has great advantages for studying phenomena such as global- and rate-remapping in both grid and place cells.

References

1. Tolman, E.C.: Cognitive maps in animals and man. Psychologival Review 55, 189–208 (1948)
2. O'Keefe, J., Dostrovsky, J.: The hippocampus as a spatial map. preliminary evidence from unit activity in the freely-moving rat. Brain Research 34(1), 171–175 (1971)
3. Hafting, T., Fyhn, M., Molden, S., Moser, M.B., Moser, E.I.: Microstructure of a spatial map in the entorhinal cortex. Nature, 801–806 (2005)
4. Hjorth-Simonsen, A., Jeune, B.: Origin and termination of the hippocampal perforant path in the rat studied by silver impregnation. J. Comp. Neurol, 215–231 (1972)
5. Engel, J.: Epilepsy: A Comprehensive Textbook in Three Volumes. Lippincott Williams & Wilkins, Philadelphia (2008)
6. Guanella, A., Verschure, P.F.J.: A model of grid cells based on a path integration mechanism. In: Kollias, S.D., Stafylopatis, A., Duch, W., Oja, E. (eds.) ICANN 2006. LNCS, vol. 4131, pp. 740–749. Springer, Heidelberg (2006)
7. Yoon, K., Buice, M.A., Barry, C., Hayman, R., Burgess, N., Fiete, I.R.: Specific evidence of low-dimensional continuous attractor dynamics in grid cells. Nat Neurosci (2013)
8. Alonso, A., Garcia-Austt, E.: Neuronal sources of theta rhythm in the entorhinal cortex of the rat. Exp Brain Res (1987)
9. Akam, T., Oren, I., Mantoan, L., Ferenczi, E., Kullmann, D.: Oscillatory dynamics in the hippocampus support dentate gyrus-ca3 coupling. Nature Neuroscience (2012)
10. Samsonovich, A., McNaughton, B.L.: Attractor map model of the hippocampus. J. Neurosci. 17(15) (1997)
11. Lallee, S., Dominey, P.F.: Multi-modal convergence maps: From body schema and self-representation to mental imagery. Adaptive Behavior (2013)
12. Bermudez, S.: `http://sergibermudez.blogspot.com.es/p/ants-downloads.html`
13. Metta, G., Fitzpatrick, L., Natale, P., Natale, L.: Yarp: yet another robot platform. Journal on Advanced Robotics Systems (Special Issue on Software Development and Integration in Robotics) (2006)
14. Rennó-Costa, C., Lisman, J.E., Verschure, P.F.M.J.: The mechanism of rate remapping in the dentate gyrus. Neuron 68(6), 1051–1058 (2010)